

Discovery, Biological Evaluation, and Structure–Activity Relationship of Amidine Based Sphingosine Kinase Inhibitors

Thomas P. Mathews,[†] Andrew J. Kennedy,[†] Yugesh Kharel,[‡] Perry C. Kennedy,[‡] Oana Nicoara,^{§,||} Manjula Sunkara,[‡] Andrew J. Morris,[‡] Brian R. Wamhoff,^{§,||} Kevin R. Lynch,[‡] and Timothy L. Macdonald^{*,†,‡}

[†]University of Virginia, Department of Chemistry, P.O. Box 400319, McCormick Road, Charlottesville, Virginia 22904, [‡]University of Virginia, Department of Pharmacology, 1340 Jefferson Park Avenue, Charlottesville, Virginia 22908, [§]University of Virginia, Department of Medicine, Cardiovascular Division, ^{||}The Robert M. Berne Cardiovascular Research Center, Charlottesville, Virginia 22908, and [‡]University of Kentucky, Department of Internal Medicine, Lexington, Kentucky 40506

Received September 23, 2009

Sphingosine 1-phosphate (S1P), a potent phospholipid growth and trophic factor, is synthesized in vivo by two sphingosine kinases. Thus these kinases have been proposed as important drug targets for treatment of hyperproliferative diseases and inflammation. We report here a new class of amidine-based sphingosine analogues that are competitive inhibitors of sphingosine kinases exhibiting varying degrees of enzyme selectivity. These inhibitors display K_I values in the submicromolar range for both sphingosine kinases and, in cultured vascular smooth muscle cells, decrease S1P levels and initiate growth arrest.

Introduction

Sphingosine kinases 1 and 2 (SphK1 and 2)^a catalyze the phosphorylation of *D-erythro* sphingosine to form sphingosine 1-phosphate (S1P).¹ The sphingosine kinases control, in large part, the equilibrium between the survival factor, S1P, and its pro-apoptotic metabolic precursor, ceramide.² S1P has been demonstrated to be a potent agonist at five membrane-bound G-protein coupled receptors, known as S1P_{1–5},³ whose roles in physiologic and pathophysiologic states are currently under investigation. The most well understood receptor subtype, S1P₁, is now recognized as the receptor responsible for the antiapoptotic properties of S1P and is also implicated in the control of lymphocyte trafficking.⁴ Because of their regulation of S1P production, SphKs1 and 2 have been proposed to be important small molecule drug targets.⁵

SphK null mice, small interfering RNAs, and small molecule inhibitors have provided insight into the physiologic importance of these enzymes. *Sphk1*^{-/-} and *Sphk2*^{-/-} mice develop normally, while the double null genotype is embryonic lethal at midgestation.⁶ While these data suggest a compensatory mechanism for SphK1 and 2, their unequal distribution in cellular compartments,⁷ SphK1's high degree of inducibility,⁸ and SphK2's *pro-apoptotic* BH3 domain^{9,10} have led researchers to view the SphK isoforms as unequal with respect to their roles in hyperproliferative disease states. In support of this long-standing hypothesis, Spiegel and co-workers demonstrated the effectiveness of a recently developed SphK1 selective inhibitor in the treatment of an animal model of leukemia.¹¹ However, another report indicated that

manipulation of SphK2 might also be important in preventing neoplastic disease progression.¹² Studies such as these demonstrate the importance of both sphingosine kinase types in disease. However, the study of dual SphK inhibitors is under-represented in the chemical literature. A recent report in this journal documented the effectiveness of a dual inhibitor in U937 cells and its potential as a future mode of therapy.¹³

We sought to add to this growing pool of inhibitors by synthesizing a novel class of dual sphingosine kinase inhibitors. Turning to examples from the chemical literature, we noticed that conventional methods of kinase inhibition involve the use of adenosine analogues to target the ATP binding site. Although this strategy has been successful,¹⁴ the ATP binding site can be similar across a wide array of kinases and such inhibitors are often burdened by a lack of selectivity and off-target effects. In terms of sphingosine kinases, the amino acid sequence of the ATP binding domain of SphK1 and 2 is conserved across a number of diacylglycerol (DAG) kinase family members, rendering the established ATP-targeting strategy particularly problematic.

While characterizing previously reported SphK substrates, we discovered a class of sphingosine-like dual SphK1/2 inhibitors. Herein we document the effectiveness of targeting the sphingosine-binding domain of the sphingosine kinases by creating a series of amidine-based, SphK1/2 inhibitors including molecules with affinity constants of less than 1 μ M. We also demonstrate an SAR strategy that was effective in improving potency and selectivity between SphK1 and 2. These inhibitors are effective in depressing S1P levels in cultured cells and initiate growth arrest in proliferating smooth muscle cells.

Results

Initial Inhibitor Design. The initial design of substrate-based SphK1/2 inhibitors required an understanding of

*To whom correspondence should be addressed. Phone: 434-924-7718. Fax: 434-982-2302. E-mail: tlm@virginia.edu.

^aAbbreviations: S1P, sphingosine 1-phosphate; SphK1, sphingosine kinase type 1; SphK2, sphingosine kinase type 2; DAG, diacylglycerol; SAR, structure–activity relationship; S1P_n ($n = 1 - 5$), sphingosine 1-phosphate receptor subtype.

previously evaluated SphK substrates. We and others have documented that the immunomodulatory investigational drug, fingolimod (FTY720), is inactive until phosphorylated by Sphk2.^{15–17} FTY720-P is a potent agonist at the SIP receptors, most prominently the SIP₁ receptor.¹³ FTY720 has been shown to be efficacious in clinical trials of remitting relapsing multiple sclerosis.¹⁸ We have examined the receptor selectivity and metabolism of a number of classes of FTY720 analogues.^{19–22} Despite continuing interest in their role as cell-signaling entities, the SAR associated with sphingosine analogues as SphK substrates (particularly substrates of SphK1) has remained largely undefined. However, a recent study from our laboratories involving the design and evaluation of a series of heterocyclic amino alcohols as SphK substrates provided insight into the structural requirements necessary for phosphorylation. Although synthetic analogues of sphingosine phosphorylated by both SphKs are rare, we previously reported (*R*)-2-amino-2-(5-(4-octylphenyl)-1,2,4-oxadiazol-3-yl)propan-1-ol (**VPC45129**) as an amino-alcohol substrate possessing such activity.²³ We postulated that if the hydroxyl portion of this substrate were deleted, creating the (*S*)-deoxy-5-phenyl-1,2,4-oxadiazole (**1**), an efficient substrate-based dual inhibitor of the SphKs could be created (Figure 1).

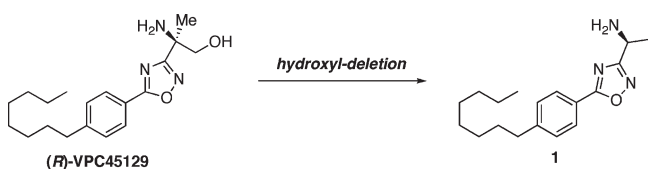
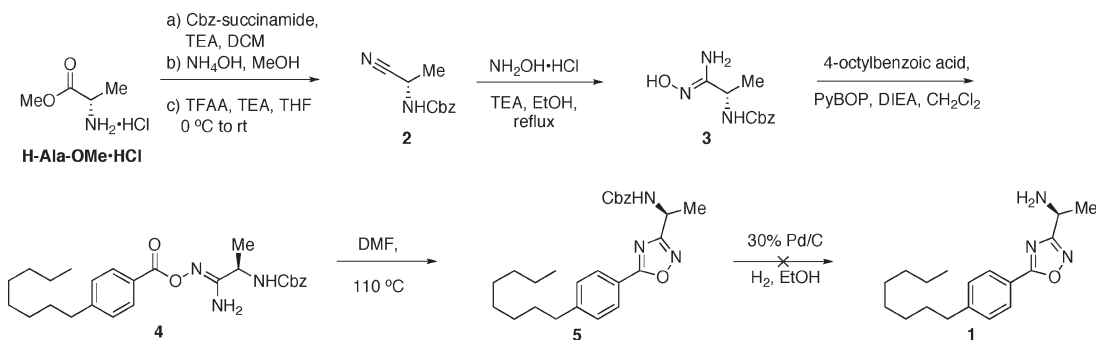
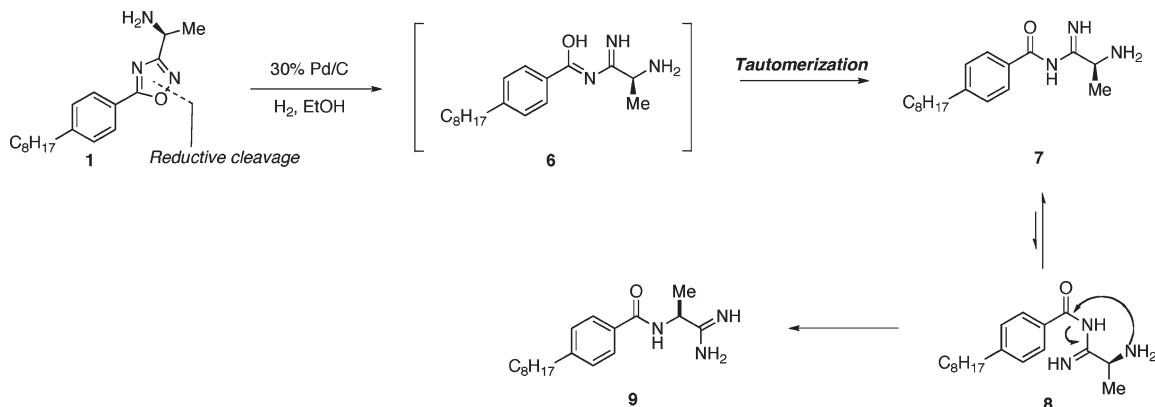


Figure 1. *R* enantiomer of **VPC45129** and its *deoxy* counterpart, **1**.

Scheme 1. Synthesis of the 5-Phenyl-1,2,4-oxadiazole **1**



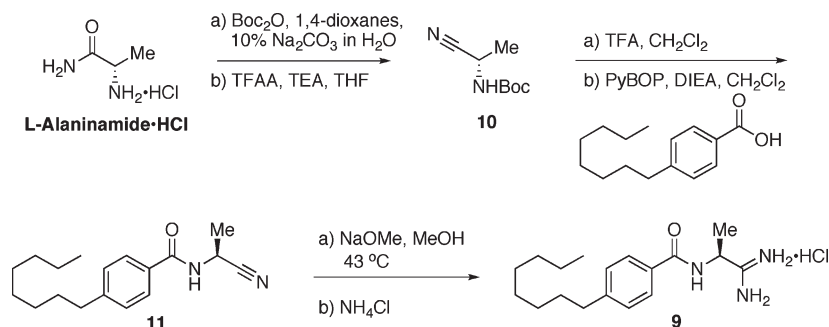
Scheme 2. Reductive Ring-Opening and Rearrangement of **1**

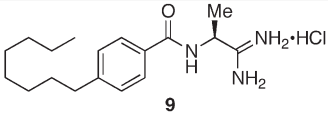


Synthesis of 1. Envisioning the stereochemistry of the amine to be readily available from *L*-alanine, the synthesis of **1** commenced the *N*-Cbz protection of the amino acid (Scheme 1). Aqueous ammonium hydroxide in methanol were used to convert the methyl ester to the corresponding amide, although a reaction time of 72 h was necessary for moderate yields. The primary amide was then converted to the nitrile **2** through a trifluoroacetic anhydride mediated dehydration. Hydroxylamine hydrochloride and triethylamine in refluxing ethanol then provided the amide-oxime **3**. In our previously cited study on heterocyclic amino alcohols as SphK substrates, we showed that amide-oximes such as **3** are excellent substrates for PyBOP mediated couplings, providing an efficient route to precursors of phenyl-1,2,4-oxadiazole systems.²³ Utilizing this methodology, **4** was synthesized, which upon heating in DMF in the presence of molecular sieves, afforded **5** in more than 80% yield.

The final deprotection of **5** could be achieved using standard palladium hydrogenolysis conditions, yielding **1** as the free amine. Surprisingly, after 15 h under these conditions, several products were present by TLC analysis. Isolation of the major product proved to be more difficult than anticipated. Thus, only small amounts of material were recovered from the deprotection of **5** (Scheme 2).

Reductive Cleavage of 1,2,4-Oxadiazole Yielding a Primary Amidine. On the basis of analytical LCMS spectra, the mass of **1** was inconsistent with that of the desired product, indicating a reduction beyond that of the *N*-Cbz group had taken place. After a search through the chemical literature, an example was found showing catalytic palladium hydrogenolysis conditions, similar to those used in the deprotection of **5**, catalyzed the *N*-O bond cleavage of phenyl-substituted 1,2,4-oxadiazoles.²⁴ Applying this model

Scheme 3. Synthesis of the Primary Amidinium Chloride **9****Table 1.** **9** Activity at SphK1 and SphK2

	K_i at SphK1	K_i at SphK2
	55 μ M	20 μ M

to our system, we hypothesized that a reduction of **1** would lead to a rapid tautomerization to the acyl-amidine **7**. After bond isomerization to the *E* isomer, **8**, a rearrangement yielding **9** was possible.

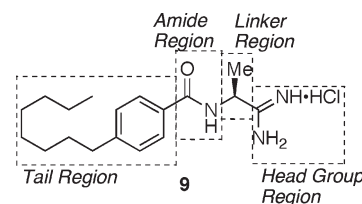
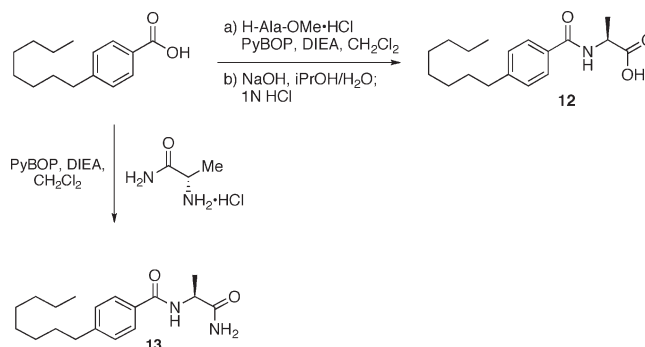
Primary Amidine Synthesis Verifies Rearrangement. To verify the rearrangement, the primary amidine **9** was independently synthesized via a separate synthetic sequence for comparison of LCMS and NMR spectra (Scheme 3). Because amidines can be easily generated from a nitrile precursor,^{25,26} synthesis of the desired product would be quite similar to that of **1**. Stirring the protected alanine methyl ester in ammonium hydroxide for 72 h proved an inefficient means of generating the amide precursor necessary in the synthesis of **2**. To circumvent this process, the *N*-Boc protection of *L*-alaninamide hydrochloride initiated the synthesis of the primary amidine.

Deprotection and coupling of **10** proved challenging as alkylation of the nitrile by the *tert*-butyl cation generated in the deprotection was a consistent problem. Limiting the formation of the alkylated-nitrile side product was achieved by closely monitoring reaction times of the trifluoroacetic acid mediated deprotection of **10** and immediately coevaporating excess solvent with diethyl ether. Coupling of the TFA salt of **10** to 4-octylbenzoic acid proceeded in relatively low yields to form the amide **11**. Limited amide formation was most likely the result of steric hindrance about the α -carbon of the amine.

As mentioned, an existing literature procedure for the formation of amidines from nitriles made amidine products very accessible. However, slow formation of the transient imidate precursor made mild heating necessary to ensure moderate product formation. After addition of ammonium chloride, the amidinium salt **9** was recovered as a white solid on precipitation with ethyl acetate.

The target-directed synthesis of amidine **9**, verified the cleavage and rearrangement of the 5-phenyl-1,2,4-oxadiazole based on NMR, LCMS, and HRMS analysis. When this compound was evaluated at the SphKs (Table 1), it was found to be a moderately potent dual inhibitor, displaying K_i values in the midmicromolar range.

Structure–Activity Relationship of 9. Realizing the potential of a dual SphK inhibitor, we focused on optimizing **9**.

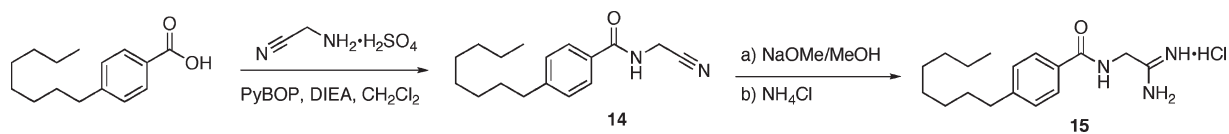
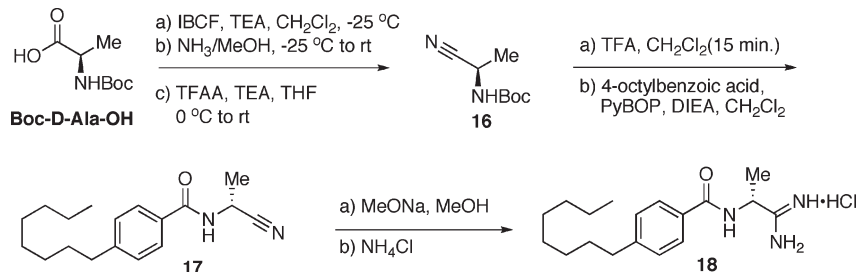
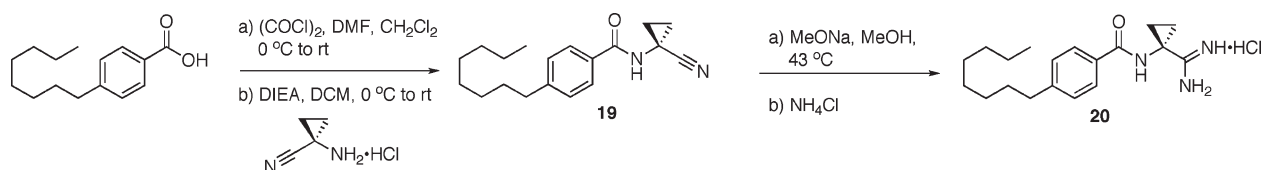
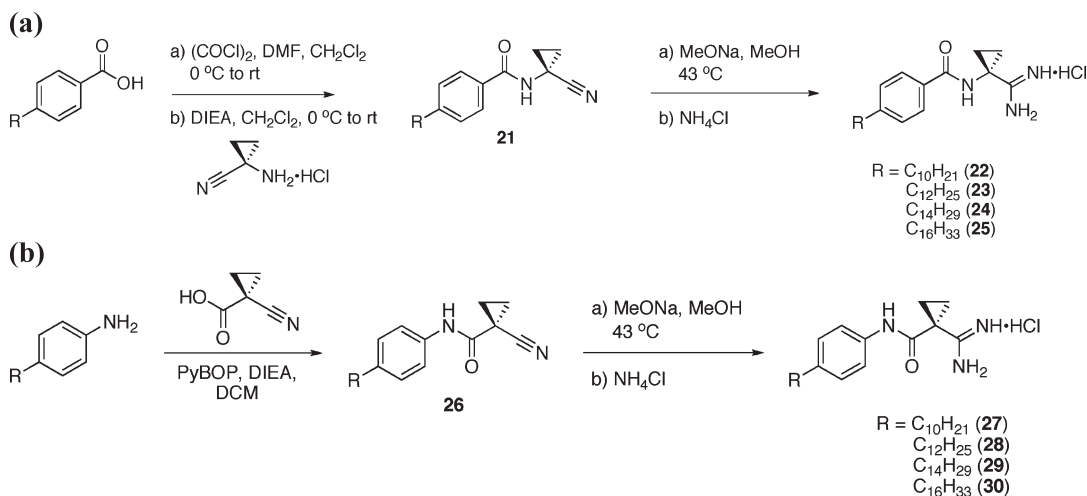
**Figure 2.** SAR regions of **9**.**Scheme 4.** Synthesis of Head Group Analogues **12** and **13**

With this in mind, our lead compound was divided into four distinct regions for SAR evaluation (Figure 2).

Head Group and Linker Region Analogues. The first region studied was the headgroup of **9**. To determine if the unique chemistry of the amidine was critical to the function of **9**, the moiety was replaced with a carboxylic acid to yield **12** and a primary amide **13** (Scheme 4).

A small set of analogues was envisioned to probe the steric and stereochemical requirements for potent SphK inhibition by amidine-based inhibitors. To better understand the steric requirements for sphingosine kinase inhibition, **14** was constructed through a PyBOP mediated amide coupling and converted to the corresponding amidine, **15** (Scheme 5).

Inversion of the stereocenter in the linker region of **9** was easily achieved by starting with *D*-alanine. Isobutylchloroformate (IBCF) followed by ammonia in methanol was found to be a facile route for the conversion of the carboxylic acid to the primary amide en route to the nitrile **16**.²⁷

Scheme 5. Synthesis of Linker Region Analogue 15**Scheme 6. Synthesis of Linker Region Analogue 18****Scheme 7. Synthesis of Linker Region Analogue 20****Scheme 8. (a) Synthesis of Tail Region Analogues 22, 23, 24, and 25; (b) Synthesis of Inverse Amide Tail Region Analogues 27, 28, 29, 30**

Subsequent deprotection and coupling afforded the benzamide 17, which was easily converted to the amidine resulting in the *R* stereoisomer of 9, 18 (Scheme 6).

Finally, to increase steric bulk in the linker region, a cyclopropyl ring was installed in place of the methyl group on 9. Synthesis of this derivative was achieved through the conversion of 4-octylbenzoic acid to the corresponding acid chloride, which was immediately coupled to 1-amino-1-cyclopropanecarbonitrile hydrochloride to provide the benzamide 19. Despite increased activation of the acyl chloride, amide formation in the presence of the cyclopropyl ring was extremely sluggish and yields of 30–40% were common. On the use of standard conditions, 20 was isolated as a white solid (Scheme 7).

Tail Region and Amide Region Analogues. To determine the optimal tail length for analogues of 9, a number of

cyclopropyl derivatives with differing tail lengths were evaluated. Amide coupling conditions in the synthesis of these derivatives were identical to that of 20 (Scheme 8).

Finally, the amide region of 9 was inverted to determine the importance of this portion of the lead molecule. Starting with an aniline derivative and 1-cyano-1-cyclopropane, PyBOP was used to synthesize the corresponding aryl-amide. Amide coupling reactions to form the reversed amide cyclopropyl scaffold were significantly improved over the previously described amide series, most likely due to a decrease in steric bulk about the nucleophilic amine. After isolation of the amide, standard conditions yielded the corresponding amidines. (Scheme 8a).

Direct in Vitro Evaluation of Sphingosine Kinase Inhibitors at SphK 1 and 2. We determined the *K*₁ values of each inhibitor at recombinant SphK1 and SphK2 (see Experimental

Section for details). As documented in the Table, the K_I values ranged from 0.2 to greater than 100 μM (i.e., no inhibition observed when inhibitor was included at 50 μM). The inhibitors appeared to be competitive, that is, inclusion of the inhibitor increased the K_M , but did not lower the V_{max} values for D-erythro-sphingosine. Data are displayed in tabular format to show the experimental K_I values for the amidine-based inhibitors at SphK1 and SphK2. We also show the experimental K_I values as a ratio to the experimental K_M of sphingosine to indicate inhibitor potency and selectivity at the sphingosine kinases (Table 2).

To test for specificity, the two most potent inhibitors (**23**, **28**) were tested at several recombinant diacylglycerol kinases (types γ , $\delta 1$, ζ) and no inhibition was observed at concentrations up to 100 μM (not shown). Many sphingosine analogues, such as DMS, have been shown to act as inhibitors of members of the protein kinase C family of enzymes. Thus, we evaluated the same two inhibitors at PKC α and observed no inhibition at concentrations up to 10 μM .

In Vitro Evaluation of SphK Inhibitors in Smooth Muscle Cells. SphK1 has been described as an immediate-early response gene in many cell types. In vascular smooth muscle cells, activation of the S1P $_1$ receptor by S1P can result in smooth muscle cell proliferation and growth. Indeed, previous studies with compounds developed by our group to target S1P receptors documented that selective inhibition of the S1P1 receptor prevented S1P-induced vascular smooth muscle cell proliferation/growth in vitro and in vivo.²⁸ In parts A and B of Figure 3, respectively, we show that serum (10% FBS) induces vascular smooth muscle cell Sphk1 mRNA and SphK1 activity while SphK2 mRNA and activity was unchanged. Serum stimulation also increases smooth muscle cell proliferation and growth. We tested the hypothesis that serum-induced smooth muscle cell proliferation was regulated in part by Sphk1. Cells were pretreated with **9** and the enantiomer **18** for 30 min and then stimulated with 10% serum for 24 h. **9** blocked serum-induced changes in S1P intracellular concentration (Figure 3C). **9**, not **18**, also blocked smooth muscle cell proliferation ($\text{EC}_{50} \sim 10 \mu\text{M}$, Figure 3D). As documented in Figure 3E, **9** was not cytotoxic to the cells on visual microscopic inspection. A cell viability assay was performed; this revealed that **9** did not induce cytotoxicity/death (Figure 3F).

Discussion

The sphingosine kinases control, in part, the cellular equilibrium of the pro-survival lipid S1P and its pro-apoptotic precursor ceramide, and the ratio of these two contrasting metabolites has been proposed to be critical to the proliferation, survival, and death of cells.²⁹ This hypothesis predicts a role for the SphKs in hyperproliferative disease models. The highly inducible nature of SphK1 mRNA and enzyme activity has focused most attention on this SphK type,⁸ but a recent literature report indicates that SphK2 is the key kinase isoform in macrophage polarization to an anticancer phenotype.¹² Such contrasting data suggests that dual and selective SphK inhibitors are needed to better characterize the relative role of these lipid kinase types.

Perhaps the most distinct structural aspect of **9** was the amidine head group. We immediately wished to understand the role this unique functional group played in sphingosine kinase inhibition. Realizing that basic amines are critical for substrate recognition by the SphKs,³⁰ and that a well-known

alkyl amidine, Distamycin A, was reported to have a $\text{p}K_a$ of 11.6 in water and DMSO,³¹ we postulated that a highly basic amidines was critical to SphK inhibition. To test this hypothesis, a carboxylic acid (**12**) and primary amide (**13**) derivatives were synthesized. Both are similar in size and shape to the amidine but negatively charged or neutral at a physiological pH. After evaluation at the SphKs, there was no inhibition observed in either case at concentrations up to 100 μM . We concluded that the unique electrostatic properties associated with amidines in an aqueous environment are critical to the function of **9** and its ilk.

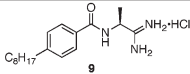
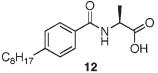
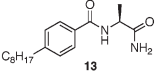
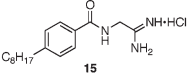
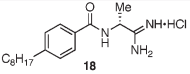
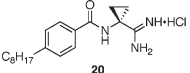
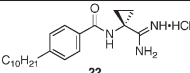
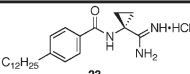
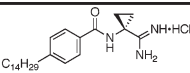
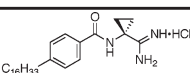
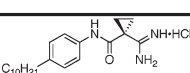
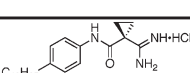
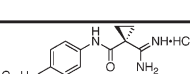
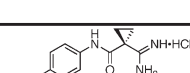
In the initial design of **1**, we considered a previous study of the SphKs³⁰ that identified aspartic acid residues in the substrate-binding domain that are critical to recognition of the basic amine in sphingosine. As a result, there is a high degree of stereoselectivity associated with substrates of the sphingosine kinases including analogues of the pro-drug **FTY720**, which are prominent SphK2 substrates.¹⁶ Interestingly, D-(+)-threo-sphingosine, wherein the amine displays stereochemistry opposite that of the natural substrate, has been found to be a weak inhibitor of the SphKs.³² Indeed, in our own study of heterocyclic amino-alcohol substrates, R-enantiomers of the imidazole analogues were found to be the most active kinase substrates, reinforcing this concept of stereoselective kinase recognition.²³ Presuming the same stereochemical preference existed for the other racemic amino-alcohols studied, this relative stereochemistry influenced the stereochemistry of our initial target **1**.

After the unexpected palladium catalyzed reductive ring-opening and rearrangement of **1** to yield the primary amidine, **9**, we directed our efforts to the elucidation of the stereochemical preference of kinase inhibition. Evaluation of the enantiomer, **18**, at both kinases revealed that inversion of stereochemistry in the linker region significantly influenced the activity profile, building in selectivity at SphK2 over SphK1. Although previously demonstrated to be important in neoplastic disease,¹² SphK2 has been described as being pro-apoptotic. However, a lack of potent inhibitors of this SphK isoform prevents further understanding of this enzyme in such disease models. The unique activity associated with **18** makes this ligand a candidate for future scaffolds of SphK2 selective inhibitors to elucidate the role of this kinase in disease.

Understanding that inversion of stereochemistry affected kinase selectivity, we next directed our attention to determining how the deletion of stereochemistry affected the potency and selectivity of our inhibitors. Such an approach would invariably impact the steric bulk in the linker region of this class of SphK inhibitors. The achiral **15** was devoid of steric bulk in the linker region and displayed a substantial loss of kinase inhibition at SphK1, although weak inhibition at SphK2 was retained. Eliminating chirality and increasing steric bulk in the case of the **20** resulted in enhanced potency at SphK1 with no change in SphK2, thus improving activity as a dual inhibitor. After establishing the influence of sterics in the linker region on SphK inhibition, this scaffold was carried forward in the analysis of tail region SAR.

Realizing the tail region of our lead compound was significantly smaller than that of the natural substrate, sphingosine, we postulated that increasing linear size in this region of the molecule would optimize kinase inhibition. The amidine **23**, having a tail region 12 carbon atoms with the cyclopropyl head group, displayed nanomolar potencies at both kinases. Comparing the K_I/K_M ratios of **23** at SphK1 and 2 shows only slight selectivity toward SphK1. The amidines **24** and **25**

Table 2. The Binding Constants for D-erythro-Sphingosine Were Measured in the Presence (K'_M) or Absence (K_M) of a Fixed Concentration (0.1–50 μ M) of a VPC Compound (I)^a

	K_I (μ M) <i>SphK1</i>	K_I (μ M) <i>SphK2</i>	K_I/K_M (<i>SphK1</i>)	K_I/K_M (<i>SphK2</i>)
Sphingosine (K_M)	10	5	—	—
 9	55	20	5.5	4
 12	>100	>100	>10	>20
 13	>100	>100	>10	>20
 15	> 100	60	> 10	12
 18	> 100	25	> 10	5
 20	25	23	2.5	4.6
 22	5	4	0.5	0.8
 23	0.2	0.5	0.02	0.1
 24	10	32	1	6.4
 25	36	10	3.6	2
 27	3	4	0.3	0.8
 28	0.3	6	0.03	1.2
 29	8.4	> 100	0.8	> 20
 30	30	> 100	3	> 20

^a K_I values were calculated using the equation: $K_I = [I]/(K'_M/K_M - 1)$.

demonstrated the limits to alkyl chain length, as these analogues having 14 and 16 carbon atoms displayed a steep decrease in inhibitory activity. Such a result is most likely due to the size of the hydrophobic pocket in the substrate-binding domain of the kinases.

Inversion of the benzamide region of the molecule provided the most compelling results in terms of kinase selectivity. Overall, a similar trend of alkyl group length and potency was observed with the inverted benzamides. Potency at the SphKs was increased at a length of 12 carbons but decreased

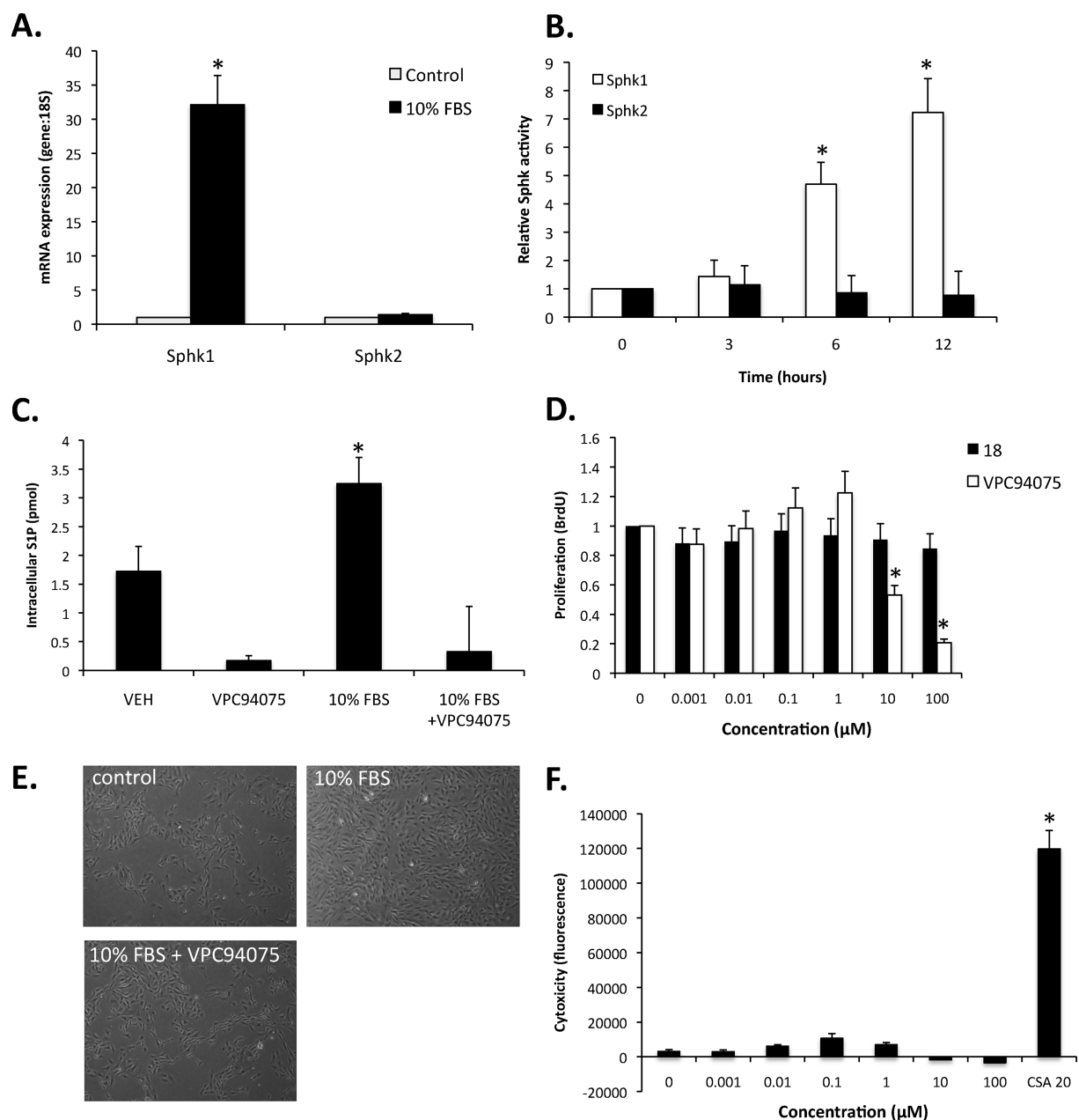


Figure 3. Inhibition of Sphk1 with **9** prevents serum-induced smooth muscle cell proliferation. (A) Quantitative real-time PCR analysis of Sphk1 and Sphk2 mRNA normalized to 18S mRNA following 4 h of serum (10% FBS) stimulation ($N = 3$). (B) Sphk1 and Sphk2 activity ($[^{32}\text{P}]\text{-S1P}$) following 0, 3, 6, and 12 h of 10% FBS stimulation ($N = 3$). (C) Changes in intracellular S1P concentration (C17 S1P) measured by LC/MS following 12 h of 10% FBS stimulation ($N = 2$). (D) Dose-response of **18** and **9** on smooth muscle cell incorporation of BrdU in response to 24 h 10% FBS stimulation ($N = 6$). (E) Light microscopy images (20 \times magnification) in control, 10% FBS-treated and 10% FBS + **9** (10 μM). (F) Cytotoxic response to **9** (0.001–100 μM) and 20 μM cyclosporine A (CSA) as measured by the Promega MultiTox-Fluor assay ($N = 3$). * denotes $P < 0.05$, N denotes biological replicate; mean \pm standard deviation.

with 14 and 16 carbons. Most intriguing was the selectivity this series displayed to SphK1. The amidine **28**, the 12-carbon analogue, displayed a dramatic degree of selectivity for SphK1 with potencies of 0.3 μM at SphK1 and 6 μM at SphK2. Comparing the K_I/K_M ratios of **28** at SphK1 and 2 showed that the analogue displayed 40-fold selectivity for SphK1 over SphK2. Much like **18**, **28** displayed unforeseen selectivity that could serve as a template for future classes of selective, amidine-based SphK inhibitors. Such compounds, if active in vivo, could be useful in testing hypotheses of the relative roles of SphK types in hyperproliferative diseases.

Plasma levels of S1P are reported as being in the high nanomolar range, typically between 200 and 800 nM.³³ While

cellular levels of sphingolipids, a group that exists in a myriad of forms, are typically considered to be approximately an order of magnitude higher.³⁴ Not surprisingly, the observed K_M of the sphingosine kinases for sphingosine is approximately 10 μM and 5 μM for SphK1³⁵ and SphK2,³⁶ respectively. Consequently, previously described selective SphK inhibitors exhibiting seemingly poor K_I values have been effective at lowering cellular S1P production and proliferation. While such inhibitors have proven quite effective at elucidating the role of the sphingosine kinases in various disease states, the relatively high dosages required for such inhibitors renders their therapeutic index unfavorable. At the outset of this study, we hoped to identify a new class of

sphingosine kinase inhibitors that would be effective both in cells and in vivo with a therapeutic index that would eliminate the likelihood of drug toxicity. While the amidine-containing compounds identified in this study have improved potency over reported sphingosine kinase inhibitors, they are largely charged at physiologic pH, leading us to consider whether such molecules could penetrate cells. Evaluation of our lead compound **9** at vascular smooth muscle cells has demonstrated that amidine-based sphingosine kinase inhibitors are effective at lowering overall S1P levels in these cells, correlating with a decrease in cell proliferation. Currently, efforts are underway to better characterize the more potent amidine-based inhibitors in a number of disease models.

Conclusions

At the outset of this study, we sought to synthesize a *deoxy* 5-phenyl-1,2,4-oxadiazole derivative of a previously described SphK1 and SphK2 dual substrate. After an unexpected palladium catalyzed ring-opening and rearrangement, a new amidine-based sphingosine kinase inhibitor, **9**, was developed that displayed moderate potencies as an inhibitor of SphK1 and SphK2. Demonstration of the effectiveness of a moderate inhibitor in a smooth muscle cell based hyperproliferative disease model illustrates the potential of this new class of sphingosine kinase inhibitors to answer long-standing questions on the pharmacology of the sphingosine kinases. We have identified a potent dual SphK inhibitor (**23**), a potent selective SphK1 inhibitor (**28**), and a moderately potent SphK2 selective inhibitor (**18**). Most importantly, we have begun to identify the pharmacophore associated with amidine-based sphingosine kinase inhibitors that we hope to exploit in future SphK inhibitors active in vivo.

Experimental Section

General Synthetic Materials and Methods. All nonaqueous reactions were carried out in oven or flame-dried glassware under an argon or nitrogen atmosphere with dry solvents and magnetic stirring, unless otherwise stated. The argon and nitrogen were dried by passing through a tube of Drierite. Anhydrous diethyl ether (Et₂O), toluene, dichloromethane (CH₂Cl₂), methanol (MeOH), tetrahydrofuran (THF), and *N,N*-dimethylformamide (DMF) were purchased from Aldrich or VMR Chemicals and used as received. THF was dried over activated molecular sieves (4 Å) prior to use. All other reagents were purchased from Acros chemicals and Aldrich chemicals. Except as indicated otherwise, reactions were monitored by thin layer chromatography (TLC) using 0.25 mm Whatman precoated silica gel plates. Flash chromatography was performed with the indicated solvents and Dynamic Adsorbents silica gel (particle size 0.023–0.040 mm). Proton (¹H) and carbon (¹³C) NMR spectra were recorded on a Varian UnityInova 500/51 or Varian UnityInova 300/54 at 300 K unless otherwise noted. Chemical shifts are reported in ppm (δ) values relative to the solvent as follows: CDCl₃ (δ 7.24 for proton and δ 77.0 for carbon NMR), DMSO-*d*₆ (δ 2.50 for proton and δ 39.5 for carbon NMR), CD₃OD (δ 3.31 for proton and δ 47.6 for carbon NMR). All high-resolution mass spectrometry was carried out by the High-Resolution Mass Spectrometry Facility in the School of Chemical Sciences at the University of Illinois Urbana—Champaign (Urbana, IL).

General Procedure A: Conversion of Nitriles to Amidines. A nitrile (0.21 mmol) was taken up in 2.1 mL of anhydrous methanol; 42 μL of a solution of 0.5 M sodium methoxide in methanol was immediately added. This mixture was allowed to stir for 15 h at 43 °C, at which time 0.231 mmol of ammonium chloride was added to the reaction, while still stirring at this

elevated temperature. When the reaction appeared complete by TLC, the mixture was allowed to cool to ambient temperature and the solution was evaporated to dryness. The crude material was next taken up in chloroform and filtered through a fine fritted funnel. The eluent was collected and thoroughly dried under vacuum. Finally, the reaction mixture was taken up in ethyl acetate and filtered again through a fine fritted funnel; the product was recovered as a white or off-white crystalline solid.

General Procedure B: PyBOP Mediated Couplings of Amines, Anilines, and Amide Oximes to Carboxylic Acids. To a suspension of an amine (0.43 mmol) in anhydrous DCM (4.3 mL) was added the acid (0.43 mmol) and PyBOP (0.43 mmol). Finally, diisopropylethylamine (1.72 mmol) was added and the reaction was allowed to stir for 15 h. At this time, the reaction mixture was evaporated to dryness and reconstituted in 100 mL of EtOAc. The solution was extracted with four 10 mL portions of 1N HCl followed by one 10 mL portion of brine. The organic layer was dried with MgSO₄ and evaporated to dryness. The crude organic material was purified by flash chromatography.

General Procedure C: Conversion of Carboxylic Acids to Acyl Chlorides. A carboxylic acid (0.28 mmol) and a catalytic amount of dimethylformamide were dissolved in dichloromethane (2.8 mL), and the solution was cooled to 0 °C. Oxalyl chloride (0.84 mmol) was added dropwise, and the reaction mixture was warmed to room temperature. After stirring for 2 h, the solution was evaporated to dryness; the crude material was taken up in three 1 mL portions of diethyl ether and immediately evaporated. The oil was dried under vacuum for an additional 30 min and carried on for alkylation by an amine.

General Procedure D: Alkylation of Acyl Chlorides by Amines. To a stirring solution of a primary amine (1.68 mmol) in DCM (8.5 mL) was added an acyl chloride (2.184 mmol) as a solution in an additional volume of DCM (8.5 mL). The mixture was then cooled to 0 °C, and diisopropylethyl amine (5.04 mmol) was added dropwise. The reaction mixture was allowed to warm to ambient temperature slowly and stirred for an additional 15 h. At this time, the reaction mixture was evaporated to dryness and reconstituted in ethyl acetate (150 mL). The solution was extracted with three 15 mL portions of 1N HCl followed by one 15 mL portion of brine. The organic layer was then dried with MgSO₄, filtered through a fritted funnel, and dried to an oil. The crude mixture was purified via flash chromatography.

General Procedure E: Conversion of a Primary Amide to a Nitrile. A primary amide (9.3 mmol) and triethylamine (18.9 mmol) was taken up in 93 mL of anhydrous THF and cooled to 0 °C. Upon cooling, trifluoroacetic anhydride (11.16 mmol) was added dropwise to the reaction mixture; after 10 min of stirring at this low temperature, the reaction mixture was allowed to warm to ambient temperature and evaporated to dryness. The crude organic mixture was taken up in 250 mL of EtOAc and extracted with four 15 mL portions of 1N HCl followed by one 10 mL portion of brine. The organic layer was then dried with MgSO₄ and evaporated to an oil.

General Procedure F: Trifluoroacetic Acid Mediated Deprotection of *N*-Boc Protected Amines. To a stirring solution of the *N*-Boc protected amino-nitrile (1.2 mmol) in anhydrous DCM (12 mL) was added TFA, dropwise (12 mL) at room temperature. After 15 min, the reaction mixture was evaporated to dryness. Three 5 mL portions of diethyl ether were then added and immediately evaporated to yield the trifluoroacetate salt as an off-white solid. The salts were dried under high vacuum for a minimum of 1 h before being carried forth.

(S)-1-(5-(4-Octylphenyl)-1,2,4-oxadiazol-3-yl)ethanamine (1). Compound **5** (0.43 mmol) was dissolved in wet ethanol (20 mL) and to this solution was added approximately 200 mg of activated palladium on carbon (30% w/w). The ambient atmosphere was then replaced with hydrogen and stirred for 15 h. After this time, the reaction mixture was filtered through celite and concentrated to an oil. After purification by column chromatography (15–20% MeOH in CHCl₃), **1** was recovered as an

off-white solid (0.06 mmol). ^1H NMR (500 MHz, DMSO) δ 9.05 (bs, 3H), 8.94 (d, $J = 6.2$, 1H), 7.91 (d, $J = 8.1$, 2H), 7.28 (d, $J = 7.9$, 2H), 4.75–4.64 (m, 1H), 2.61 (t, $J = 7.6$, 2H), 1.56 (dd, $J = 6.9$, 14.1, 1H), 1.50 (d, $J = 7.2$, 3H), 1.31–1.14 (m, 10H), 0.83 (t, $J = 6.9$, 3H). ^{13}C NMR (126 MHz, DMSO) δ 172.94, 166.97, 146.99, 130.96, 128.53, 128.36, 47.57, 40.45, 40.28, 40.11, 39.95, 39.78, 39.61, 39.45, 35.40, 31.71, 31.18, 29.24, 29.11, 29.04, 22.52, 18.83, 14.41. LCMS and HRMS data was identical to **9**.

(S)-Benzyl 1-Cyanoethylcarbamate (2). General procedure E was used to convert 5.7 mmol of *N*-Cbz-alaninamide to the title product. After flash chromatography, 4.9 mmol of product was recovered. ^1H NMR (500 MHz, CDCl_3) δ 7.50–7.30 (m, 5H), 5.15 (s, 2H), 4.75–4.61 (m, 1H), 1.56 (d, $J = 7.2$, 3H). ^{13}C NMR (126 MHz, CDCl_3) δ 154.87, 135.50, 128.66, 128.53, 128.32, 119.14, 67.72, 38.08, 19.55.

(S,Z)-Benzyl 1-Amino-1-(hydroxyimino)propan-2-ylcarbamate (3). The intermediate **2** (4.7 mmol) was dissolved in anhydrous ethanol (7.5 mL). To this solution was added triethylamine (10.81 mmol) and hydroxylamine hydrochloride (10.34 mmol). The reaction mixture was heated to reflux for three hours, after which time it was concentrated to an oil and reconstituted in dichloromethane (150 mL). The organic layer was washed with three 10 mL portions of water and one 10 mL portion of brine. The organic solution was dried over MgSO_4 and evaporated to dryness. Purification by flash chromatography yielded 2.3 mmol of **3** as an off-white solid. ^1H NMR (500 MHz, CD_3OD) δ 7.45–7.22 (m, 5H), 5.07 (s, 2H), 4.21 (q, $J = 7.0$, 1H), 1.34 (d, $J = 7.1$, 3H). ^{13}C NMR (126 MHz, CD_3OD) δ 156.56, 156.27, 136.78, 128.04, 127.58, 127.45, 66.13, 18.11.

(R,Z)-Benzyl 1-Amino-1-(4-octylbenzoyloxyimino)propan-2-ylcarbamate (4). General procedure B was used to couple **4** (2.1 mmol) to 4-octylbenzoic acid. After column chromatography, 1.6 mmol of the title product was recovered as a white solid. ^1H NMR (300 MHz, CDCl_3) δ 7.93 (d, $J = 8.2$, 2H), 7.35 (s, 5H), 7.25 (d, $J = 7.2$, 3H), 5.41–5.22 (m, 3H), 5.12 (s, 2H), 4.5–3.8 (m, 1H), 2.71–2.61 (m, 2H), 1.69–1.53 (m, 5H), 1.31–1.26 (m, 9H), 0.86 (t, $J = 6.7$, 3H). ^{13}C NMR (126 MHz, CDCl_3) δ 164.08, 159.49, 156.77, 148.73, 135.92, 129.45, 128.55, 128.30, 128.07, 126.83, 67.25, 48.22, 36.03, 31.85, 31.15, 29.42, 29.26, 29.22, 22.65, 17.66, 14.11.

(S)-Benzyl 1-(5-(4-Octylphenyl)-1,2,4-oxadiazol-3-yl)ethylcarbamate (5). The intermediate **4** (1.5 mmol) was dissolved in DMF (30 mL). One g of activated 4 Å molecular sieves were added and the reaction mixture was heated to 110 °C. After 6 h, the mixture was cooled to ambient temperature and filtered through a medium frit. After diluting with 250 mL of ethyl acetate, the solution was extracted with eight 15 mL portions of water and one 15 mL portion of brine. The organic layer was collected, dried over MgSO_4 , and evaporated to dryness. Purification by flash chromatography yielded 1.14 mmol of **5**. ^1H NMR (300 MHz, CDCl_3) δ 8.01 (d, $J = 8.3$, 2H), 7.41–7.28 (m, 7H), 5.42 (d, $J = 8.6$, 1H), 5.26–5.04 (m, 2H), 2.78–2.60 (m, 2H), 1.74–1.51 (m, 5H), 1.32–1.25 (m, 10H), 0.88 (t, $J = 6.8$, 3H). ^{13}C NMR (126 MHz, CDCl_3) δ 176.26, 171.80, 155.46, 148.69, 136.21, 129.17, 128.53, 128.14, 121.37, 67.01, 44.24, 36.08, 31.84, 31.09, 29.41, 29.22, 22.66, 20.72, 14.12.

(S)-N-(1-Amino-1-iminopropan-2-yl)-4-octylbenzamide Hydrochloride (9). General procedure A was used to convert 0.24 mmol of **12** to the title product. After previously described recrystallization techniques, 0.078 mmol of a white powdery product was recovered. ^1H NMR (500 MHz, DMSO) δ 8.91 (bs, 1H), 8.66 (d, $J = 5.2$, 1H), 7.86 (d, $J = 8.1$, 2H), 7.29 (d, $J = 8.1$, 3H), 7.17 (bs, 1H), 4.65–4.47 (m, 1H), 2.61 (t, $J = 7.6$, 2H), 1.56 (dd, $J = 6.9$, 14.1, 2H), 1.47 (d, $J = 7.2$, 3H), 1.32–1.14 (m, 10H), 0.83 (t, $J = 6.8$, 3H). ^{13}C NMR (126 MHz, DMSO) δ 172.75, 167.26, 147.07, 130.91, 128.54, 128.35, 47.91, 35.39, 31.70, 31.21, 29.23, 29.02, 22.52, 18.64, 14.41. LCMS: $t_{\text{R}} = 8.4$ min; $m/z = 304$, 607 (dimer). HRMS m/z calcd for $\text{C}_{18}\text{H}_{30}\text{N}_3\text{O}$ ($M + \text{H}$), 304.2389; found, 304.2384.

(S)-tert-Butyl 1-Cyanoethylcarbamate (10). Sodium carbonate (1.5 g) was dissolved in 15 mL of water, and to this solution was added alaninamide hydrochloride (5.7 mmol). In a separate flask, di-*tert*-butyl dicarbonate (11.4 mmol) was dissolved in 1,4-dioxanes (11.4 mL). This organic solution was then added to the aqueous solution and allowed to stir for 15 h. After this time, the reaction mixture was diluted with 25 mL of 1N HCl and extracted with four 25 mL portions of ethyl acetate. The organic layers were combined, washed with brine, dried over MgSO_4 , and concentrated to a white solid. This solid was then subjected to general procedure E. After flash chromatography, 3.1 mmol of the title product was recovered. ^1H NMR (500 MHz, CDCl_3) δ 4.82 (bs, 1H), 4.62 (bs, 1H), 1.54 (d, $J = 7.2$, 3H), 1.46 (s, 8H). ^{13}C NMR (126 MHz, CDCl_3) δ 154.10, 119.53, 37.57, 28.21, 19.62.

(S)-N-(1-Cyanoethyl)-4-octylbenzamide (11). General procedure F was used to deprotect **10** (1.17 mmol). After standard purification techniques, the off-white solid was coupled to 4-octylbenzoic acid (1.17 mmol) using general procedure B. Flash chromatography yielded 0.5 mmol of the title product. ^1H NMR (500 MHz, CDCl_3) δ 7.70 (d, $J = 8.1$, 2H), 7.25 (dd, $J = 4.0$, 7.8, 2H), 6.56 (bs, 1H), 5.16 (p, $J = 7.2$, 1H), 2.64 (t, $J = 6.4$, 2H), 1.65 (ddd, $J = 9.5$, 10.2, 19.7, 5H), 1.42–1.15 (m, 10H), 0.87 (dd, $J = 5.9$, 7.0, 3H). ^{13}C NMR (126 MHz, CDCl_3) δ 166.58, 148.04, 129.94, 128.80, 127.18, 119.40, 36.24, 35.85, 31.83, 31.13, 29.39, 29.21, 22.63, 19.58, 14.08.

(S)-2-(4-Octylbenzamido)propanoic Acid (12). General procedure B was used to couple 0.31 mmol of L-alanine methyl ester to 4-octylbenzoic acid. After standard work up procedures, the recovered material was dissolved in 5 mL of isopropyl alcohol. In a separate flask, 0.62 mmol of sodium hydroxide was dissolved in 2 mL of water and poured into isopropyl alcohol solution. The mixture was heated to 60 °C for 3 h, at which time the reaction mixture was cooled to ambient temperature and evaporated to dryness. The crude material was taken up in 50 mL of a 4:1 suspension of ethyl acetate to 1N HCl. The aqueous layer was extracted three additional times with ethyl acetate. The organic layers were combined, washed with brine, and dried over magnesium sulfate. Evaporation of solvent yielded 0.23 mmol of the title product as an off-white solid. ^1H NMR (300 MHz, CDCl_3) δ 7.71 (d, $J = 8.2$ Hz, 2H), 7.31–7.16 (m, 3H), 6.80 (d, $J = 6.9$ Hz, 1H), 4.81–4.77 (m, 1H), 2.76–2.51 (m, 2H), 1.57 (d, $J = 7.1$ Hz, 5H), 1.27 (d, $J = 7.3$ Hz, 11H), 0.87 (t, $J = 6.7$ Hz, 3H). ^{13}C NMR (75 MHz, CDCl_3) δ 176.41, 168.48, 147.81, 131.10, 129.06, 127.39, 48.95, 36.08, 32.07, 30.81, 29.24, 23.00, 18.37, 14.32.

(S)-N-(1-Amino-1-oxopropan-2-yl)-4-octylbenzamide (13). General procedure B was used to couple 0.42 mmol of L-alaninamide hydrochloride to 4-octylbenzoic acid. After standard work up and purification procedures, 0.23 mmol of the title product was recovered. ^1H NMR (500 MHz, CD_3OD) δ 7.79 (d, $J = 8.5$ Hz, 2H), 7.28 (d, $J = 8.2$ Hz, 2H), 4.56 (q, $J = 7.2$ Hz, 1H), 2.67 (t, $J = 7.5$ Hz, 2H), 1.66–1.60 (m, 2H), 1.47 (d, $J = 7.2$ Hz, 3H), 1.37–1.19 (m, 10H), 0.89 (t, $J = 7.0$ Hz, 3H). ^{13}C NMR (126 MHz, CD_3OD) δ 176.59, 168.54, 147.05, 131.15, 128.13, 127.16, 49.26, 35.32, 31.59, 28.97, 22.29, 16.88, 13.00.

N-(Cyanomethyl)-4-octylbenzamide (14). General procedure B was used to couple aminoacetonitrile bisulfate (0.42 mmol) to 4-octylbenzoic acid. After flash chromatography, 0.38 mmol of the title product was recovered. ^1H NMR (300 MHz, CDCl_3) δ 7.70 (d, $J = 8.3$, 2H), 7.25 (d, $J = 7.6$, 2H), 6.78 (t, $J = 5.5$, 1H), 4.37 (d, $J = 5.8$, 2H), 2.64 (t, $J = 9$, 2H), 1.62 (dt, $J = 7.4$, 22.1, 2H), 1.3–1.26 (m, 10H), 0.87 (t, $J = 6.7$, 2H). ^{13}C NMR (75 MHz, CDCl_3) δ 174.80, 148.82, 130.03, 129.08, 127.46, 117.30, 77.67, 77.25, 76.83, 36.09, 32.06, 31.35, 29.62, 29.44, 28.19, 22.86, 14.31.

N-(2-Amino-2-iminoethyl)-4-octylbenzamide Hydrochloride (15). General procedure A was used to convert 0.38 mmol of **14** to the title product. Upon isolation with standard purification techniques, 0.16 mmol of the title product was recovered as

a white solid. ^1H NMR (500 MHz, DMSO) δ 8.94 (s, 1H), 7.82 (d, $J = 8.0$, 4H), 7.29 (d, $J = 7.9$, 2H), 4.15 (d, $J = 5.2$, 2H), 2.61 (t, $J = 7.4$, 2H), 1.68–1.47 (m, 2H), 1.25–1.21 (m, $J = 10\text{H}$), 0.83 (t, $J = 6.4$, 3H). ^{13}C NMR (126 MHz, DMSO) δ 168.79, 167.52, 147.03, 130.99, 128.61, 128.17, 35.39, 31.70, 31.17, 29.23, 29.10, 29.02, 22.51, 14.40. LCMS: $t_{\text{R}} = 6.9$ min; $m/z = 290$. HRMS m/z calculated for $\text{C}_{17}\text{H}_{28}\text{N}_3\text{O}$ (M + H), 290.2232; found, 290.2232.

(*R*)-*tert*-Butyl 1-Cyanoethylcarbamate (16). To a stirring solution of *N*-Boc-D-alanine (7.9 mmol) in dichloromethane (16 mL) was added triethylamine (35.55 mmol). This solution was cooled to $-25\text{ }^\circ\text{C}$, and isobutyl chloroformate (15.8 mmol) was added dropwise. The reaction was stirred at this low temperature for 45 min, at which time ammonia (23.7 mmol) as a 7N solution in methanol was added and the reaction mixture and was allowed to warm to ambient temperature and stirred for an additional 15 h. After this time, the reaction mixture was concentrated to an oil by rotary evaporation and reconstituted in ethyl acetate (200 mL). The organic layer was washed with four 20 mL portions of 1N HCl and one 15 mL portion of brine and dried over MgSO_4 . The solvent was evaporated, and the intermittent product was dried under vacuum. General procedure E was then used to convert the primary amide to a nitrile. Four mmol of the title product was recovered as a white powdery solid. ^1H and ^{13}C spectral data was identical to that of **10**.

(*R*)-*N*-(1-Cyanoethyl)-4-octylbenzamide (17). General procedure F was used to deprotect **16** (1.7 mmol). General procedure B was then used to couple the resulting amine to 4-octylbenzoic acid. After standard purification techniques, the title product (0.85 mmol) was recovered. ^1H and ^{13}C spectral data were identical to that of **11**.

(*R*)-*N*-(1-Amino-1-iminopropan-2-yl)-4-octylbenzamide Hydrochloride (18). General procedure A was used to convert **17** (0.38 mmol) to the title product. After standard purification techniques, **18** (0.15 mmol) was recovered as a white solid. ^1H and ^{13}C spectral data were identical to that of **9**. LCMS: $t_{\text{R}} = 8.4$ min; $m/z = 304$. HRMS m/z calculated for $\text{C}_{18}\text{H}_{30}\text{N}_3\text{O}$ (M + H), 304.2389; found, 304.2382.

***N*-(1-Cyanocyclopropyl)-4-octylbenzamide (19).** General procedure C was used to convert 4-octylbenzoic acid (0.53 mmol) to the corresponding acyl chloride. After standard workup procedures, the acyl-chloride was coupled to 1-amino-1-cyclopropyl-carbonitrile hydrochloride (0.41 mmol) using general procedure D. After purification by flash chromatography, the title product (0.21 mmol) was recovered. ^1H NMR (500 MHz, CDCl_3) δ 7.69 (d, $J = 8.3$, 2H), 7.21 (d, $J = 8.4$, 2H), 7.12 (s, 1H), 2.68–2.58 (m, 2H), 1.59 (dd, $J = 5.8$, 8.3, 4H), 1.35 (dd, $J = 5.9$, 8.3, 2H), 1.32–1.20 (m, 10H), 0.87 (t, $J = 7.0$, 3H). ^{13}C NMR (126 MHz, CDCl_3) δ 168.06, 148.02, 129.96, 128.73, 127.27, 120.23, 35.85, 31.83, 31.13, 29.39, 29.21, 22.63, 20.88, 16.91, 14.08.

***N*-(1-Carbamidoylcyclopropyl)-4-octylbenzamide Hydrochloride (20).** General procedure A was used to convert **15** (0.17 mmol) to the corresponding amidine. After standard workup and purification techniques **20** (0.04 mmol) was recovered as a white solid. ^1H NMR (500 MHz, CD_3OD) δ 7.82 (d, $J = 8.3$, 2H), 7.30 (d, $J = 8.2$, 2H), 2.76–2.62 (m, 2H), 1.75 (dd, $J = 5.9$, 8.5, 2H), 1.64 (dd, $J = 7.1$, 14.3, 2H), 1.56 (dd, $J = 6.1$, 8.4, 2H), 1.29 (dd, $J = 7.1$, 15.0, 11H), 0.89 (t, $J = 7.0$, 3H). ^{13}C NMR (126 MHz, CD_3OD) δ 172.52, 169.94, 147.79, 130.21, 128.19, 127.47, 35.32, 32.59, 31.58, 30.98, 29.11, 28.97, 28.82, 22.29, 18.16, 12.99. LCMS: $t_{\text{R}} = 8.5$ min; $m/z = 316$. HRMS m/z calcd for $\text{C}_{19}\text{H}_{30}\text{N}_3\text{O}$ (M + H), 316.2389; found, 316.2381.

***N*-(1-Cyanocyclopropyl)-4-decylbenzamide (21; C10).** General procedure C was used to convert 2.184 mmol of 4-decylbenzoic acid to the corresponding acyl chloride. After work up, this intermediate was immediately subjected to methods described in general procedure D in the presence of 1-amino-1-cyclopropanecarbonitrile hydrochloride (1.68 mmol). After flash chromatography, 1 mmol of the title product was recovered as a white

solid. ^1H NMR (500 MHz, CDCl_3) δ 7.70 (dd, $J = 3.2$, 8.1, 2H), 7.21 (d, $J = 8.0$, 2H), 2.66–2.58 (m, 2H), 1.59 (d, $J = 5.6$, 4H), 1.36 (q, $J = 5.8$, 2H), 1.32–1.20 (m, 15H), 0.87 (t, $J = 6.9$, 3H). ^{13}C NMR (126 MHz, CDCl_3) δ 168.16, 148.04, 129.96, 128.74, 127.32, 120.30, 35.86, 31.88, 31.15, 29.59, 29.45, 29.31, 29.23, 22.67, 20.88, 16.91, 14.12.

***N*-(1-Cyanocyclopropyl)-4-dodecylbenzamide (21; C12).** General procedure C was used to convert 4-dodecylbenzoic acid (0.52 mmol) to the corresponding acyl chloride. After standard work up procedures, the intermediate was immediately subjected to conditions described in general procedure D in the presence of 1-amino-1-cyclopropanecarbonitrile hydrochloride (0.4 mmol). After flash chromatography, 0.15 mmol of the title product was recovered. ^1H NMR (500 MHz, CDCl_3) δ 7.68 (d, $J = 7.1$, 2H), 7.23 (d, $J = 7.5$, 2H), 6.82 (s, 1H), 2.63 (t, $J = 7.7$, 2H), 1.65–1.57 (m, 4H), 1.35 (t, $J = 7.0$, 2H), 1.29–1.25 (m, 17H), 0.88 (t, $J = 6.5$, 3H). ^{13}C NMR (126 MHz, CDCl_3) δ 167.81, 148.06, 130.01, 128.75, 127.19, 120.07, 35.85, 31.89, 31.11, 29.61, 29.53, 29.42, 29.32, 29.20, 22.66, 20.88, 16.97, 14.08.

***N*-(1-Cyanocyclopropyl)-4-tetradecylbenzamide (21; C14).** Tetradecanoic acid (0.61 mmol) was subjected to the methods described in general procedure C. After standard work up procedures were used, the intermediate acyl chloride was coupled to 1-amino-1-cyclopropanecarbonitrile hydrochloride (0.47 mmol) using general procedure D. After flash chromatography, 0.28 mmol of the title product was isolated. ^1H NMR (300 MHz, CDCl_3) δ 7.68 (d, $J = 8.2$, 2H), 7.23 (d, $J = 8.2$, 2H), 6.85 (s, 1H), 2.63 (t, $J = 9$, 2H), 1.64–1.55 (m, 4H), 1.35 (dd, $J = 5.8$, 8.5, 2H), 1.25 (s, 20H), 0.87 (t, $J = 6.6$, 3H). ^{13}C NMR (75 MHz, CDCl_3) δ 168.05, 148.30, 130.19, 128.98, 127.43, 120.32, 36.09, 32.15, 31.38, 29.88, 29.68, 29.58, 29.45, 22.92, 21.10, 17.20, 14.36.

***N*-(1-Cyanocyclopropyl)-4-hexadecylbenzamide (21; C16).** General procedure C was used to convert hexadecanoic acid (0.58 mmol) to the corresponding acyl chloride. After standard work up techniques, the intermediate was coupled to 1-amino-1-cyclopropanecarbonitrile hydrochloride using the methods described in general procedure D. Upon flash chromatography 0.41 mmol of the title product was recovered. ^1H NMR (500 MHz, CDCl_3) δ 7.68 (d, $J = 8.2$, 2H), 7.23 (d, $J = 8.1$, 2H), 6.81 (s, 1H), 2.63 (t, $J = 7.7$, 3H), 1.64–1.58 (m, 4H), 1.35 (q, $J = 4.9$, 2H), 1.33–1.21 (m, 27H), 0.88 (t, $J = 6.9$, 3H). ^{13}C NMR (126 MHz, CDCl_3) δ 167.79, 148.06, 130.01, 128.75, 127.19, 120.07, 97.26, 35.84, 31.90, 31.11, 29.66, 29.63, 29.54, 29.43, 29.33, 29.20, 22.67, 20.88, 16.96, 14.08.

***N*-(1-Carbamidoylcyclopropyl)-4-decylbenzamide Hydrochloride (22).** General procedure A was used to convert **21; C10** (0.12 mmol) to the corresponding amidine. After standard recrystallization techniques, 0.026 mmol of the title product was recovered. ^1H NMR (500 MHz, CD_3OD) δ 7.81 (d, $J = 6.1$, 2H), 7.30 (d, $J = 6.3$, 2H), 2.67 (t, $J = 6.7$, 2H), 1.75 (s, 2H), 1.63 (s, 2H), 1.56 (s, 2H), 1.29 (d, $J = 20.9$, 14H), 0.89 (dd, $J = 4.5$, 7.0, 3H). ^{13}C NMR (126 MHz, CD_3OD) δ 172.51, 169.93, 147.78, 130.20, 128.34, 128.04, 127.48, 35.32, 32.59, 31.63, 30.97, 29.27, 28.81, 28.66, 22.30, 18.15, 12.98. LCMS: $t_{\text{R}} = 10.34$; $m/z = 344$. HRMS m/z calcd for $\text{C}_{21}\text{H}_{34}\text{N}_3\text{O}$ (M + H), 344.2702; found, 344.2698.

***N*-(1-Carbamidoylcyclopropyl)-4-dodecylbenzamide Hydrochloride (23).** General procedure A was used to convert **21; C12** (0.15 mmol) to the corresponding amidine. Upon previously described recrystallization procedures 0.06 mmol of the title product was recovered. ^1H NMR (500 MHz, DMSO) δ 9.08 (s, 1H), 8.66 (bs, 4H), 7.81 (d, $J = 6.7$, 2H), 7.27 (d, $J = 6.9$, 2H), 2.60 (s, 2H), 1.65 (s, 2H), 1.54 (s, 2H), 1.37 (s, 2H), 1.21 (s, 19H), 0.83 (s, 3H). ^{13}C NMR (126 MHz, DMSO) δ 172.22, 167.99, 147.01, 131.21, 128.45, 128.32, 35.38, 33.09, 31.74, 31.23, 29.45, 29.27, 29.16, 28.98, 22.54, 18.42, 14.42. LCMS: $t_{\text{R}} = 10.85$ min; $m/z = 372$. HRMS m/z calcd for $\text{C}_{23}\text{H}_{38}\text{N}_3\text{O}$ (M + H), 372.3015; found, 302.3005.

***N*-(1-Carbamimidoylcyclopropyl)-4-tetradecylbenzamide Hydrochloride (24)**. General procedure A was used to convert 0.26 mmol of **21**; **C14** to the corresponding amidine. After standard recrystallization techniques, 0.04 mmol of the title product was recovered as a white solid. ¹H NMR (500 MHz, DMSO) δ 9.04 (s, 1H), 8.61 (bs, 4H), 7.81 (d, *J* = 7.8, 2H), 7.27 (d, *J* = 5.8, 2H), 2.60 (t, *J* = 7.1, 2H), 1.65 (s, 2H), 1.54 (d, *J* = 5.5, 2H), 1.37 (s, 2H), 1.24–1.21 (m, 21H), 0.83 (t, *J* = 6.5, 3H). ¹³C NMR (126 MHz, DMSO) δ 172.23, 168.02, 147.03, 131.24, 128.45, 128.31, 127.93, 35.38, 33.12, 31.72, 31.20, 29.44, 29.25, 29.13, 28.98, 22.52, 18.40, 14.39. LCMS: *t*_R = 12.3 min; *m/z* = 400. HRMS *m/z* calcd C₂₅H₄₂N₃O (M + H), 400.3328; found, 400.3322.

***N*-(1-Carbamimidoylcyclopropyl)-4-hexadecylbenzamide Hydrochloride (25)**. General procedure A was used to convert 0.18 mmol of **21**; **C16** to the corresponding amidine. However, instead of methanol, ethanol was used to solubilize the starting material. After standard recrystallization techniques, 0.04 mmol of the title product was recovered as a white solid. ¹H NMR (500 MHz, DMSO) δ 9.06 (s, 1H), 8.65 (bs, 4H), 7.81 (d, *J* = 7.5, 2H), 7.27 (d, *J* = 7.5, 2H), 2.67–2.56 (m, 2H), 1.65 (s, 2H), 1.54 (d, *J* = 4.0, 2H), 1.37 (s, 2H), 1.21 (bs, 25H), 0.84 (t, *J* = 5.4, 3H). ¹³C NMR (126 MHz, DMSO) δ 172.16, 168.01, 147.02, 131.21, 128.45, 128.31, 35.38, 33.11, 31.74, 31.24, 29.46, 29.27, 29.15, 28.99, 22.54, 18.41, 14.42. LCMS: *t*_R = 12.4; *m/z* = 428. HRMS *m/z* calcd C₂₇H₄₆N₃O (M + H), 428.3641; found, 428.3642.

1-Cyano-*N*-(4-decylphenyl)cyclopropanecarboxamide (26; C10). General procedure B was used to couple 4-decylaniline (1.00 mmol) to 1-cyanocyclopropanecarboxylic acid. After column chromatography, 0.99 mmol of the title product was recovered as a white solid. ¹H NMR (300 MHz, CDCl₃) δ 8.16 (s, 1H), 7.41 (d, *J* = 8.4 Hz, 2H), 7.14 (d, *J* = 8.4 Hz, 2H), 2.73–2.40 (m, 2H), 1.77 (dd, *J* = 8.2, 4.4 Hz, 2H), 1.68–1.51 (m, 4H), 1.29 (d, *J* = 10.1 Hz, 14H), 0.90 (t, *J* = 6.6 Hz, 3H). ¹³C NMR (75 MHz, CDCl₃) δ 163.54, 140.27, 134.81, 129.13, 120.87, 120.27, 35.63, 32.16, 31.69, 29.86, 29.75, 29.60, 29.49, 22.95, 18.44, 14.39, 14.32.

1-Cyano-*N*-(4-dodecylphenyl)cyclopropanecarboxamide (26; C12). General procedure B was used to couple 4-dodecylaniline (1.00 mmol) to 1-cyanocyclopropanecarboxylic acid. After column chromatography, 0.99 mmol of the title product was recovered as a white solid. ¹H NMR (300 MHz, CDCl₃) δ 8.18 (s, 1H), 7.41 (d, *J* = 8.3 Hz, 2H), 7.14 (d, *J* = 8.3 Hz, 2H), 2.57 (t, *J* = 7.6 Hz, 2H), 1.83–1.67 (m, 2H), 1.67–1.45 (m, 4H), 1.28 (s, 18H), 0.90 (t, *J* = 6.4 Hz, 3H). ¹³C NMR (75 MHz, CDCl₃) δ 163.53, 140.24, 134.84, 129.12, 120.88, 120.26, 35.63, 32.19, 31.70, 29.93, 29.77, 29.63, 29.51, 22.96, 18.44, 14.40, 14.31.

1-Cyano-*N*-(4-tetradecylphenyl)cyclopropanecarboxamide (26; C14). General procedure B was used to couple 4-tetradecylaniline (1.00 mmol) to 1-cyanocyclopropanecarboxylic acid. After column chromatography, 0.99 mmol of the title product was recovered as a white solid. ¹H NMR (300 MHz, CDCl₃) δ 8.24–8.00 (m, 1H), 7.40 (d, *J* = 8.4 Hz, 2H), 7.15 (d, *J* = 8.4 Hz, 2H), 2.76–2.38 (m, 2H), 1.77 (dd, *J* = 8.2, 4.4 Hz, 2H), 1.67–1.50 (m, 4H), 1.27 (s, 22H), 0.89 (t, *J* = 6.6 Hz, 3H). ¹³C NMR (75 MHz, CDCl₃) δ 163.50, 140.32, 134.74, 129.16, 120.81, 120.28, 35.63, 32.18, 31.70, 29.93, 29.76, 29.63, 29.50, 22.95, 18.45, 14.39.

1-Cyano-*N*-(4-hexadecylphenyl)cyclopropanecarboxamide (26; C16). General procedure B was used to couple 4-hexadecylaniline (1.00 mmol) to 1-cyanocyclopropanecarboxylic acid. After column chromatography, 0.99 mmol of the title product was recovered as a white solid. ¹H NMR (300 MHz, CDCl₃) δ 8.29–7.98 (m, 1H), 7.43 (t, *J* = 14.0 Hz, 2H), 7.14 (d, *J* = 8.4 Hz, 2H), 2.78–2.44 (m, 2H), 1.77 (dd, *J* = 8.2, 4.4 Hz, 2H), 1.67–1.50 (m, 4H), 1.27 (s, 26H), 0.89 (t, *J* = 6.7 Hz, 3H). ¹³C NMR (75 MHz, CDCl₃) δ 163.50, 140.29, 134.78, 129.14, 120.83, 120.27, 35.63, 32.19, 31.71, 29.95, 29.77, 29.64, 29.51, 22.96, 18.44, 14.40.

1-Carbamimidoyl-*N*-(4-decylphenyl)cyclopropanecarboxamide Hydrochloride (27). General procedure A was used to convert 0.99 mmol of **26**; **C10** to the corresponding amidine. After standard recrystallization techniques, 0.51 mmol of the title product was recovered as a white solid. ¹H NMR (500 MHz, DMSO) δ 9.69 (s, 1H), 8.96 (s, 4H), 7.63–7.31 (m, 2H), 7.17–7.04 (m, 2H), 2.66–2.30 (m, 2H), 1.66–1.34 (m, 6H), 1.19 (dd, *J* = 30.7, 9.2 Hz, 14H), 0.90–0.76 (m, 3H). ¹³C NMR (126 MHz, DMSO) δ 168.27, 166.44, 138.41, 136.53, 128.64, 128.58, 121.33, 121.28, 34.98, 31.73, 31.44, 29.98, 29.45, 29.30, 29.13, 29.02, 22.54, 15.12, 14.41. LCMS: *t*_R = 9.8 min; *m/z* = 344. HRMS *m/z* calcd C₂₁H₃₄N₃O (M + H), 344.2702; found, 344.2690.

1-Carbamimidoyl-*N*-(4-dodecylphenyl)cyclopropanecarboxamide Hydrochloride (28). General procedure A was used to convert 0.99 mmol of **26**; **C12** to the corresponding amidine. After standard recrystallization techniques, 0.45 mmol of the title product was recovered as a white solid. ¹H NMR (300 MHz, DMSO) δ 9.57 (s, 1H), 9.16 (s, 2H), 8.91 (s, 2H), 7.45 (d, *J* = 8.1 Hz, 2H), 7.10 (d, *J* = 8.3 Hz, 2H), 2.48 (m, 2H), 1.52 (m, 6H), 1.21 (s, 18H), 0.83 (s, 3H). ¹³C NMR (75 MHz, DMSO) δ 168.33, 166.76, 138.72, 136.69, 128.88, 121.61, 35.21, 31.97, 31.67, 30.17, 29.69, 29.53, 29.39, 29.26, 22.77, 15.42, 14.65. LCMS: *t*_R = 11.5 min; *m/z* = 372. HRMS *m/z* calcd C₂₃H₃₈N₃O (M + H), 372.3015; found, 372.3011.

1-Carbamimidoyl-*N*-(4-tetradecylphenyl)cyclopropanecarboxamide Hydrochloride (29). General procedure A was used to convert 0.99 mmol of **26**; **C14** to the corresponding amidine. After standard recrystallization techniques, 0.37 mmol of the title product was recovered as a white solid. ¹H NMR (300 MHz, DMSO) δ 9.57 (s, 1H), 9.16 (s, 2H), 8.91 (s, 2H), 7.45 (d, *J* = 8.1 Hz, 2H), 7.10 (d, *J* = 8.3 Hz, 2H), 2.48 (s, 2H), 1.52 (dd, *J* = 40.8, 22.8 Hz, 6H), 1.21 (s, 22H), 0.83 (s, 3H). ¹³C NMR (75 MHz, DMSO) δ 168.33, 166.76, 138.72, 136.69, 128.88, 121.61, 35.21, 31.97, 31.67, 30.17, 29.69, 29.53, 29.39, 29.26, 22.77, 15.42, 14.65. *t*_R = 12.5 min; *m/z* = 400. HRMS *m/z* calcd C₂₅H₄₂N₃O (M + H), 400.3328; found, 400.3334.

1-Carbamimidoyl-*N*-(4-hexadecylphenyl)cyclopropanecarboxamide Hydrochloride (30). General procedure A was used to convert 0.99 mmol of **26**; **C16** to the corresponding amidine. However, instead of methanol, ethanol was used to solubilize the starting material. After standard recrystallization techniques, 0.27 mmol of the title product was recovered as a white solid. ¹H NMR (500 MHz, DMSO) δ 9.92 (s, 2H), 9.82–9.58 (s, 1H), 9.06 (s, 2H), 7.47 (s, 2H), 7.09 (s, 2H), 2.49 (s, 2H), 1.46 (d, *J* = 62.7 Hz, 6H), 1.21 (s, 26H), 0.83 (s, 3H). ¹³C NMR (75 MHz, DMSO) δ 168.32, 166.75, 138.71, 136.69, 128.87, 121.59, 35.21, 31.97, 31.69, 30.17, 29.70, 29.54, 29.39, 29.28, 22.78, 15.42, 14.66. *t*_R = 13.2; *m/z* = 428. HRMS *m/z* calcd C₂₇H₄₆N₃O (M + H), 428.3641; found, 428.3639.

Sphingosine Kinase Assay. Human SphK1 and mouse SphK2 cDNAs were used to generate mutant baculoviruses that encoded these proteins. Infection of Sf9 insect cells with the viruses for 72 h resulted in >1000-fold increases in SphK activity in 10000g supernatant fluid from homogenized cell pellets. The enzyme assay conditions were exactly as described,¹⁶ except infected Sf9 cell extract containing 2–3 μg protein was used as a source of enzyme.

Vascular Smooth Muscle Cell Bioassays. Rat aortic vascular smooth muscle cells were cultured in vitro as previously described.²⁸ Total mRNA was extracted using Trizol (Invitrogen), cDNA was synthesized using the iScript cDNA synthesis kit (BioRad), and quantitative real-time polymerase chain reaction (PCR) was used to measure Sphk1, Sphk2, and 18S mRNA expression as previously described.²⁷ Primer sequences: Sphk1 F: GTGCCATCCAGAAACCCCTA, R: AGTCCACGTCA-GCAACGAAA; Sphk2 F: TGGGAAGGCATTGTCACTGT, R: AAGAAGCGAGCAGTTGAGCA; 18S F: CGGTAC-CACATCCAAGGAA, R: AGCTGGAATTACCGCGGC. Proliferation was assessed by BrdU incorporation (10 μM)

based on the Roche BrdU immuno-absorbance assay. Cytotoxic response was determined by the Promega MultiTox-Fluor Assay.

Quantification of S1P by LC/MS. S1P and DHS1P were quantified as their bisacetylated derivatives (BisAcS1P and BisAcDHS1P) using adaptations of previously reported methods.³⁷ Derivatization eliminates sample carryover that is a noted problem with these analytes. In brief, cells were washed in PBS and then scraped into 2 mL of ice cold MeOH, which was transferred to glass tubes containing 1 mL CHCl₃, 0.5 mL 0.1 M HCl, and 50 pmol of C17 S1P. After vortexing, an additional 1 mL of CHCl₃ and 1.3 mL 0.1 M HCl were added to the tubes containing the cell suspension. The tubes were vortexed a second time and centrifuged. The lipid-containing organic phase was separated into a second 4 mL glass vial. The organic layer was evaporated to dryness and the material was acetylated with acetic anhydride in pyridine. After a second evaporation, the resulting material was dissolved in MeOH for analysis. Samples were separated on an Agilent Technologies Zorbax Eclipse XDB-C8 column, 4.6 mm × 150 mm, 5 mm particle size using methanol/water/HCOOH, 79/20/0.5, v/v, with 5 mM NH₄COOH as solvent A and methanol/acetonitrile/HCOOH, 59/40/0.5, v/v, with 5 mM NH₄COOH as solvent B. Analytes were detected by electrospray ionization tandem mass spectrometry using an ABI 4000 Q-Trap instrument operated in positive ionization mode with optimized declustering potentials, collision energies, and exit potentials. The following *m/z* transitions were monitored: BisAcC17S1P 448/388; BisACS1P, 462/402; BisAcDHS1P, 464/404. Calibration curves were generated using BisAcS1P BisAcDHS1P and BisAcDHS1P that were prepared from S1P, DHS1P, and C17S1P obtained from Avanti Polar Lipids and quantified independently by phosphorus analysis.

Liquid Chromatography and Mass Spectrometry for Evaluation of Chemical Purity. All compound subjected to biological evaluation were determined to be > 95% pure by LCMS evaluation. High performance liquid chromatography–mass spectrometry (LCMS) was carried out on a Waters 2695 separations module and a Finnigan LCQ series mass spectrometer. All compounds were evaluated for purity using a Thompson Instrument Company Advantage C₁₈ column. Columns were outfitted with 5 μm beads with a 60 Å pore size; columns were 250 mm in length and 4.6 mm in diameter. Mobile phase A consisted of HPLC grade H₂O and 0.01% TFA; mobile phase B consisted of MeCN and 0.01% TFA. LCMS identification and purity utilized a binary gradient starting with 90% A and 10% B and linearly increasing to 100% B over the course of 10 min, followed by an isocratic flow of 100% B for an additional 10 min. A flow rate of 1 mL/min was maintained throughout the HPLC method. The purity of all products was determined by integration of the total ion count (TIC) spectra and integration of the ultraviolet (UV) spectra at 214 nm; a Waters 486 tunable absorbance detector was used to collect all UV data. Retention times are abbreviated as *t_R*; mass to charge ratios are abbreviated as *m/z*.

Acknowledgment. This work was supported by grants from the National Institutes of Health (R01 GM067958 to K.R.L. and T.L.M., T32 GM008715 to P.C.K.; HL081682 to B.R.W.; GM50388 to A.J.M. and American Heart Association SDG to B.R.W. We also thank Dr. Pam Schoppee-Bortz, Ph.D., Cardiovascular Division, MSTP-candidate John Hogan, predoctoral candidate Monica Lee, ME, Department of Biomedical Engineering, and Amanda M. Gellett, Department of Pharmacology, University of Virginia, for their technical expertise.

Supporting Information Available: Additional ¹H and ¹³C NMR data for **9**, **13**, **20**, and **22**. This material is available free of charge via the Internet at <http://pubs.acs.org>.

References

- Hait, N. C.; Oskeritzian, C. A.; Paugh, S. W.; Milstien, S.; Spiegel, S. Sphingosine kinases, sphingosine 1-phosphate, apoptosis and diseases. *Biochim. Biophys. Acta* **2006**, *1758*, 2016–2026.
- Spiegel, S.; Milstien, S. Sphingosine-1-phosphate: and enigmatic signaling lipid. *Nat. Rev. Mol. Cell Biol.* **2003**, *4*, 397–407.
- Lynch, K. R. Lysophospholipid Receptor Nomenclature. *Biochim. Biophys. Acta* **2002**, *1582*, 70–71.
- Rosen, H.; Sanna, M.; Germana, C.; Stuart, M.; Gonzalez-Cabrera, P. J. Tipping the gatekeeper: S1P regulation of endothelial barrier function. *Trends Immunol.* **2007**, *28*, 102–107.
- French, K. J.; Upson, J. J.; Keller, S. N.; Zhuang, Y.; Yun, J. K.; Smith, C. D. Discovery and evaluation of inhibitors of human sphingosine kinase. *Cancer Res.* **2003**, *63*, 5962–5969.
- Mizugishi, K.; Yamashita, T.; Olivera, A.; Miller, G. F.; Spiegel, S.; Proia, R. L. Essential role for sphingosine kinases in neural and vascular development. *Mol. Cell Biol.* **2005**, *25*, 11113–11121.
- Okada, T.; Ding, G.; Sonoda, H.; Kajimoto, T.; Haga, Y.; Khosrowbeygi, A.; Gao, S.; Miwa, N.; Jahangeer, S.; Nakamura, S.-I. Involvement of N-terminal-extended form of sphingosine kinase 2 in serum-dependent regulation of cell proliferation and apoptosis. *J. Biol. Chem.* **2005**, *280*, 36318–36325.
- Johnson, K. R.; Becker, K. P.; Facchinetti, M. M.; Hannun, Y. A.; Obeid, L. M. PKC-dependent activation of sphingosine kinase 1 and translocation to the plasma membrane. Extracellular release of sphingosine-1-phosphate induced by phorbol 12-myristate 13-acetate (PMA). *J. Biol. Chem.* **2002**, *277*, 35257–35262.
- Maceyka, M.; Sankala, H.; Hait, N. C.; Le Stunff, H.; Liu, H.; Toman, R.; Collier, C.; Zhang, M.; Satin, L. S.; Merrill, A. H.; Milstien, S.; Spiegel, S. SphK1 and SphK2, sphingosine kinase isoenzymes with opposing functions in sphingolipid metabolism. *J. Biol. Chem.* **2005**, *280*, 37118–37129.
- Liu, H.; Toman, R. E.; Goparaju, S. K.; Maceyka, M.; Nava, V. E.; Sankala, H.; Payne, S. G.; Bektas, M.; Ishii, I.; Chun, J.; Milstien, S.; Spiegel, S. Sphingosine kinase type 2 is a putative BH3-only protein that induces apoptosis. *J. Biol. Chem.* **2003**, *278*, 40330–40336.
- Paugh, S. W.; Paugh, B. S.; Rahmani, M.; Kapitonov, D.; Almenara, J. A.; Kordula, T.; Milstien, S.; Adams, J. K.; Zipkin, R. E.; Grant, S.; Spiegel, S. A selective sphingosine kinase 1 inhibitor integrates multiple molecular therapeutic targets in human leukemia. *Blood* **2008**, *112*, 1382–1391.
- Weigert, A.; Schiffmann, S.; Sekar, D.; Ley, S.; Menrad, H.; Werno, C.; Grosch, S.; Geisslinger, G.; Brüne, B. Sphingosine kinase 2 deficient tumor xenografts show impaired growth and fail to polarize macrophages towards and anti-inflammatory phenotype. *Int. J. Cancer* **2009**, PMID: 19618460.
- Wong, L.; Tan, S. S. L.; Lam, Y.; Melendez, A. J. Synthesis and evaluation of sphingosine analogues as inhibitors of sphingosine kinases. *J. Med. Chem.* **2009**, *52*, 3618–3626.
- Goldstein, D. M.; Gray, N. S.; Zarrinkar, P. P. High-throughput kinase profiling as a platform for drug discovery. *Nat. Rev. Drug Discovery* **2008**, *7*, 391–397.
- Mandala, S.; Hajdu, R.; Bergstrom, J.; Quackenbush, E.; Xie, J.; Milligan, J.; Thornton, R.; Shei, G.-J.; Card, D.; Keohane, C.; Rosenbach, M.; Hale, J.; Lynch, C. L.; Rupprecht, K.; Parsons, W.; Rosen, H. Alteration of lymphocyte trafficking by sphingosine-1-phosphate receptor agonists. *Science* **2002**, *296*, 346–349.
- Brinkmann, V.; Davis, M. D.; Heise, C. E.; Albert, R.; Cottens, S.; Hof, R.; Bruns, C.; Prieschl, E.; Baumruker, T.; Hiestand, P.; Foster, C. A.; Zollinger, M.; Lynch, K. R. The immune modulator FTY720 targets sphingosine 1-phosphate receptors. *J. Biol. Chem.* **2002**, *277*, 21453–21457.
- Kharel, Y.; Lee, S.; Snyder, A. H.; Sheasley-O'Neill, S. L.; Morris, M. A.; Setiady, Y.; Zhu, R.; Zigler, M. A.; Burcin, T. L.; Ley, K.; Tung, K. S. K.; Engelhard, V. H.; Macdonald, T. L.; Pearson-White, S.; Lynch, K. R. Sphingosine kinase 2 is required for modulation of lymphocyte traffic by FTY720. *J. Biol. Chem.* **2005**, *280*, 36865–36872.
- Dev, K. K.; Mullershausen, F.; Mattes, H.; Kuhn, R. R.; Bilbe, G.; Hoyer, D.; Mir, A. Brain sphingosine-1-phosphate receptors: implication for FTY720 in the treatment of multiple sclerosis. *Pharmacol. Ther.* **2008**, *117*, 77–93.
- Clemens, J. J.; Davis, M. D.; Lynch, K. R.; Macdonald, T. L. Synthesis of *para*-Alkyl Aryl Amide Analogues of Sphingosine-1-Phosphate: Discovery of Potent S1P Receptor Agonists. *Bioorg. Med. Chem. Lett.* **2003**, *13*, 3401–3404.
- Clemens, J. J.; Davis, M. D.; Lynch, K. R.; Macdonald, T. L. Synthesis of 4(5)-phenylimidazole-based analogues of Sphingosine-1-Phosphate and FTY720: Discovery of Potent S1P₁ Receptor Agonists. *Bioorg. Med. Chem. Lett.* **2005**, *15*, 3568–3572.

- (21) Foss, F. W.; Snyder, A. H.; Davis, M. D.; Rouse, M.; Okusa, M. D.; Lynch, K. R.; Macdonald, T. L. Synthesis and biological evaluation of α -aminophosphonates as potent, subtype-selective sphingosine 1-phosphate receptor agonists and antagonists. *Bioorg. Med. Chem.* **2007**, *15*, 663–677.
- (22) Zhu, R.; Snyder, A. H.; Kharel, K.; Schaffter, L.; Sun, Q.; Kennedy, P. C.; Lynch, K. R.; Macdonald, T. L. Asymmetric Synthesis of Conformationally Constrained Fingolimod Analogues-Discovery of an Orally Active Sphingosine 1-Phosphate Receptor Type-1 Agonist and Receptor Type-3 Antagonist. *J. Med. Chem.* **2007**, *50*, 6428–6435.
- (23) Foss, F. W.; Mathews, T. P.; Kharel, Y.; Kennedy, P. C.; Snyder, A. H.; Davis, M. D.; Lynch, K. R.; Macdonald, T. L. Synthesis and biological evaluation of sphingosine kinase substrates as sphingosine 1-phosphate receptor prodrugs. *Bioorg. Med. Chem.* **2009**, *17*, 6123–6136.
- (24) Tyrkov, A.; Usova, A. Reduction of Substituted 5-(Nitromethyl)-3-phenyl-1, 2, 4-oxadiazoles. *Russ. J. Org. Chem.* **2004**, *40*, 286–287.
- (25) Kitagawa, H.; Ozawa, T.; Takahata, S.; Iida, M.; Saito, J.; Yamada, M. Phenylimidazole derivatives of 4-pyridone as dual inhibitors of bacterial enoyl-acyl carrier protein reductases FabI and FabK. *J. Med. Chem.* **2007**, *50*, 4710–4720.
- (26) Schaefer, F. C.; Peters, G. A. Base-Catalyzed Reaction of Nitriles with Alcohols. A Convenient Route to Imidates and Amidine Salts. *J. Org. Chem.* **1961**, *26*, 412–418.
- (27) Tang, F.-Y.; Qu, L.-Q.; Xu, Y.; Ma, R.-J.; Chen, S.-H.; Li, G. Practical Synthesis of Structurally Important Spirodiamine Templates. *Synth. Commun.* **2007**, *37*, 3793–3799.
- (28) Wamhoff, B. R.; Lynch, K. R.; Macdonald, T. L.; Owens, G. K. Sphingosine-1-phosphate receptor subtypes differentially regulate smooth muscle cell phenotype. *Arterioscler., Thromb., Vasc. Biol.* **2008**, *28*, 1454–1461.
- (29) Wymann, M. P.; Schneider, R. Lipid signalling in disease. *Nat. Rev. Mol. Cell Biol.* **2008**, *9*, 162–176.
- (30) Yokota, S.; Taniguchi, Y.; Kihara, A.; Mitsutake, S.; Igarashi, Y. Asp177 in C4 domain of mouse sphingosine kinase 1a is important for the sphingosine recognition. *FEBS Lett.* **2004**, *578*, 106–110.
- (31) Koppel, I.; Koppel, J.; Leito, I.; Grehn, L. Basicity of 3-amino-propionamidine derivatives in water and dimethyl sulphoxide. *J. Phys. Org. Chem.* **1996**, *9*, 265–268.
- (32) Buehrer, B. M.; Bell, R. M. Inhibition of sphingosine kinase in vitro and in platelets. *J. Biol. Chem.* **1992**, *267*, 3154–3159.
- (33) Lynch, K. R.; Macdonald, T. M. Sphingosine 1-phosphate chemical biology. *Biochim. Biophys. Acta* **2008**, *1781*, 508–512.
- (34) Hannun, Y. A.; Obeid, L. M. Principles of bioactive lipid signaling: lessons from sphingolipids. *Nat. Rev. Mol. Cell Biol.* **2008**, *9*, 139–150.
- (35) Olivera, A.; Kohama, T.; Tu, Z.; Milstien, S.; Spiegel, S. Purification and characterization of rat kidney sphingosine kinase. *J. Biol. Chem.* **1998**, *273*, 12576–12583.
- (36) Liu, H.; Sugiura, M.; Nava, V. E.; Edsall, L. C.; Kono, K.; Poulton, S.; Milstien, S.; Kohama, T.; Spiegel, S. Molecular cloning and functional characterization of a novel mammalian sphingosine kinase type 2 isoform. *J. Biol. Chem.* **2000**, *275*, 19513–19520.
- (37) Berdyshev, E. V.; Gorshkova, I. A.; Garcia, J. G. N.; Natarajan, V.; Hubbard, W. C. Quantitative analysis of sphingoid base-1-phosphates as bisacetylated derivatives by liquid chromatography-tandem mass spectrometry. *Anal. Biochem.* **2005**, *339*, 129–136.